

# High Frequency Wide Beam PVDF Ultrasonic Projector for Underwater Communications

M.S. Martins<sup>1,2</sup>, C. Barardo<sup>1</sup>, T. Matos<sup>1</sup>, L.M. Goncalves<sup>1</sup>, J. Cabral<sup>1</sup>, A. Silva<sup>2</sup>, S.M. Jesus<sup>2</sup>

<sup>1</sup>MEMS-UMinho, University of Minho, Campus of Azurém, Guimarães, Portugal

<sup>2</sup>LARSyS, University of Algarve Campus de Gambelas, 8005-139 Faro, Portugal  
mmartins@dei.uminho.pt

**Abstract**—This work describes the development and characterization of a wide beam and wideband ultrasonic transducer, designed as an emitter for underwater communications up to 1.5 MHz. The active element being used is composed of two layers of 110  $\mu\text{m}$  PVDF (Polyvinylidene fluoride) film, with NiCu electrodes. The transducer has a semicircular shape with a diameter of 15 cm. Pool trials show a transmitting voltage response of approximately 150 dB re  $\mu\text{Pa/V}$  @ 1m from 750kHz to 1MHz and higher than 130 dB re  $\mu\text{Pa/V}$  @ 1m between 250kHz and 1.5MHz. At 1 MHz, when excited with 12V, the transducer has a power consumption of 37.5 mW.

**Keywords**—polymer ultrasound transducer; wideband; wide beam; very high frequency; wideband digital communications; underwater wireless communications.

## I. INTRODUCTION

Underwater broadband wireless communications are well known for their limitations when compared to aerial communications. Underwater broadband communications are required for through-water high bit-rate communications for data gathering and control of permanent and mobile subsea structures as benthic labs and autonomous underwater vehicles. There are three main technologies used for underwater wireless communications: radio frequency, optical and acoustic [1].

Electromagnetic radio frequency (RF) waves are highly attenuated in subaquatic medium. RF signals are immune to acoustic noise interference and any negative effects of turbidity and bio fouling. However, radio signals are strongly attenuated when propagating through conductive medium and seawater is particularly conductive. Since, attenuation increases with frequency, its application is limited to low frequency radio. At very short distances (cm), radio can support data rates up to 1Gbps with acceptable power consumption, however at higher distances the power consumption becomes a strong constraint [2].

To address the need for higher transmission rates between underwater platforms over relatively short distances (up to 15 meters), research is mainly considering optical communications as the preferred technology. In fact, underwater communications using optical electromagnetic waves have seen significant advances recently, presenting high transfer rates with low energy consumption [3] and extremely low latencies when compared to acoustic communications. This type of systems, also called Free-space Optical (FSO) communications, consist on a light beam of the visible spectrum, to transfer information. However, underwater optical

communications are strongly dependent of water turbidity, suffering the negative effects of bio fouling and requiring a precise alignment between emitter and receiver due to the narrow-beam nature of the optic (laser) devices.

Acoustic waves propagate more easily in an aqueous environment [2] than the RF and optic waves, but the attenuation, low speed of sound, multipath, Doppler Effect and noise represents considerable obstacles in underwater wireless communications. In addition, broadband communications are limited by the typical piezoelectric ceramic acoustic transducers narrowband nature [3], and to implement an underwater broadband communication system it is required to use an ultrasonic transducer with wideband spectrum response, wide beam spreading and working in high frequency range (up to 1 MHz) [4]. Recently the use of polymeric PVDF transducers [11] arises as a promising technology to overcome the narrowband issue but its usefulness is limited given its narrow-beam nature (as the optic transducers).

This work describes the development, implementation and characterization (acoustic and electric) of a wideband and wide beam ultrasonic transducer to be used as a projector in underwater wireless communications. This transducer shows a beam spread higher than 70 degrees for a wide range of frequencies, from 250 to 1500 kHz.

This paper is organized as follows: Section 2 summarizes the basic concepts of piezoelectric transducers. Section 3 describes the material selection and the transducer design. Section 4 presents the transducer simulation using finite elements and the fabrications process. Section 5 describes the experimental setup and respective results. Finally, in Section 6, are drawn some conclusions.

## II. PIEZOELECTRIC ULTRASONIC TRANSDUCERS BACKGROUND

The spreading loss results from the dispersion of acoustic energy as it propagates in a homogeneous and infinite medium which increases with beam divergence angle and distance. The intensity of sound is equal to the pressure output power per unit area, decreasing therefore as the wave spreads out of the source [4]. The intensity quantities of interest are

$$I_0 = \frac{P_a}{A_{r0}}, \quad I = \frac{P_a}{A_r} \quad (1)$$

where,  $A_{r0}$  is the area at reference distance (1 meter),  $A_r$  is the area at distance  $r$ ,  $P_a$  is the acoustic power source,  $I_0$  is the acoustic intensity at distance  $r_0$  and  $I$  is the acoustic intensity at distance  $r$ .

The acoustic signal intensity decrease by spreading can be quantified by the spreading loss,  $g(r)$ , which is given by

$$g(r) = 10 \log \left[ \frac{I_0}{I} \right] = 10 \log \left[ \frac{A_r}{A_{r0}} \right], \quad (2)$$

Usually, at high frequencies, piezoelectric ultrasonic transducers operate in the thickness mode, which means that the deformation is along the polarization axis and the excitation electric field is in the same direction. The free displacement of the material, without restraining force and assuming uniform strain over the surface, is given by [5]

$$\xi = d_{33} \nu n \quad (3)$$

where  $\xi$  is the free displacement,  $\nu$  is the applied voltage,  $n$  is the number of layers and  $d_{33}$  is the coupling coefficient in the thickness direction. The deformation creates a pressure wave in the medium, whose force amplitude  $F$  can be obtained by [4]

$$F = A_p 2\pi c \rho f \xi \quad (4)$$

where  $c$  is the sound speed,  $\rho$  is the material density,  $A_p$  is the area of the piezoelectric element,  $f$  is the signal wave frequency and  $\xi$  is the piezoelectric material displacement.

The maximum force that the piezoelectric element can apply to a medium is obtained by:

$$F = d_{33} \frac{A_p}{S_{33}^E t_p} \nu \quad (5)$$

where  $S_{33}^E$  is the elastic compliance coefficient and  $t_p$  is the thickness of a single layer [6].

To ensure optimal operation, the force that the transducer can apply to the medium must be greater than the resulting acoustic wave force generated by the transducer deformation, otherwise, the piezoelectric material will not be able to produce a homogeneous displacement across the entire surface, generating acoustic waves with low amplitude and distortion. Through equations 4 and 5 it is possible to obtain the maximum stack thickness [7]:

$$nt_p \leq \frac{1}{2\pi c \rho S_{33}^E f} \quad (7)$$

This condition allows the calculation of the layer thickness and the number of layers for a specific frequency and material.

The acoustic beam has a pattern characterized by its divergence angle, which depends on the transducer diameter  $D$  and on the wavelength  $\lambda$ . The value of the beam divergence angle  $\delta$  is given by [4]:

$$\delta = \arcsin\left(\frac{\lambda}{D}\right) \quad (8)$$

Considering (8), for the transducer to show an omnidirectional behavior, the diameter must be smaller than the wavelength.

### III. TRANSDUCER DESIGN

The most basic and common transducer shape is the piston-type transducer, which is, basically, a piezoelectric with a disk shape. Most often those transducers are manufactured with ceramic piezoelectric materials such as: lead zirconate titanate (PZT)[8], lead titanate (PT) [9], lead magnesium niobate (PMN) [9] and lead zinc niobate (PZN) [10]. These ceramics are commonly used as resonators since they show a high piezoelectric coefficient and high acoustic impedance [11]. Besides ceramics, some other materials can be used, such as: polymers (polyvinylidene fluoride (PVDF) and P(VDF-TrFE)) [12] and single crystals (PZT, PMN and PZN) [13]. The polymeric based solutions have the lowest acoustic impedance among all materials used in underwater acoustic transducers. One of the major advantages of using low acoustic impedance is related to the high transfer of energy between the transducer and the medium, decreasing significantly the resonance effect. The resonance effect reduction has two major consequences: First, it reduces the sound pressure level output; second, it increases the transducer usable bandwidth which is desirable for broadband digital communications [7].

PVDF has a low Piezoelectric Coefficient, almost 20 times lower than common piezo ceramics [11]. Nevertheless, it is possible to overcome this limitation by suitable transducer design. Using a laminated transducer by gluing several layers of PVDF films, as presented in [11], it is possible to significantly increase the transducer performance. Another possible solution is to increase the transducer surface area but, for the piston transducer, this will reduce the beam divergence angle, according to (8). One solution to implement a wide beam transducer without compromising the acoustic power level is to use a curved surface, where the area is practically unlimited, once the transducer surface is proportional to the circumference radius, as shown in Fig. 1.

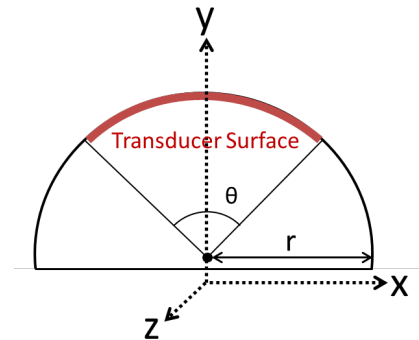


Fig. 1. Transducer 2D Model with beam spread angle of  $\theta$ .

Fig. 1 shows a cylinder shape transducer with radius  $r$ , where the transducer length (in red) is equal to the arc length in the circular sector defined by the central angle  $\theta$ .

#### IV. SIMULATION AND IMPELEMENTATION

The prototype dimensions were calculated taking into account the requirements in table 1.

TABLE I. TRANSDUCER REQUIREMENTS

Characteristics	Value
Frequency	Up to 1 MHz
Cylinder radius	7.5 cm
XY plane beam spread	70°
XZ plane beam spread	10°

Regarding (7), for a 1MHz PVDF transducer the maximum thickness is limited at 229  $\mu\text{m}$  [11]. Therefore, the selected active element has two layers of 110  $\mu\text{m}$  PVDF with NiCu electrodes [14].

According to the design in Fig 1 for a transducer to cover an area of 70° in XY plane and 10° in YZ plane when using a cylinder with 7.5 cm radius, the active element has to be 9.2 cm long and 1.7 cm wide.

##### A. Simulations

The simulation results are shown in Fig 2 for the sound pressure level (dB re 1  $\mu\text{Pa}$ ) at 750 kHz and 1.25 MHz in a symmetric axis.

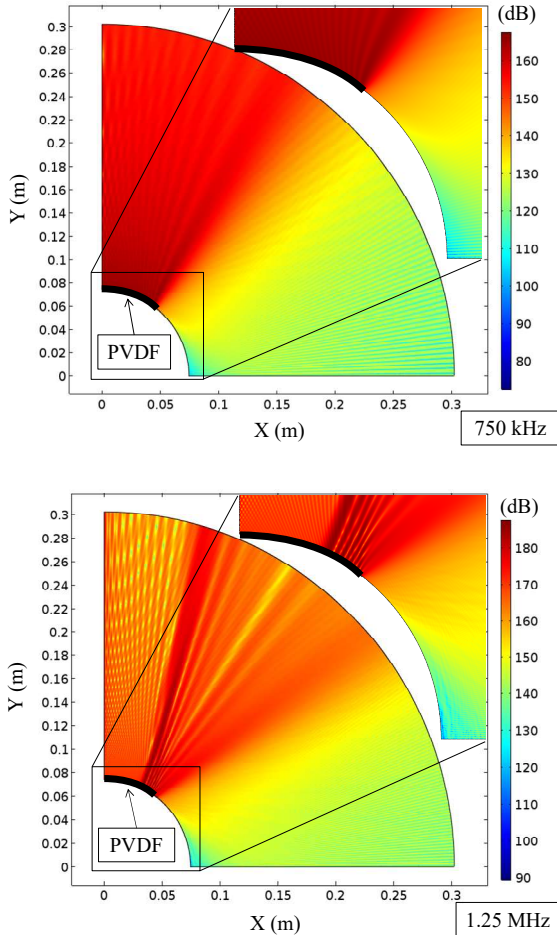


Fig. 2. FEM simulation of sound pressure level for 750 kHz and 1.25 MHz.

The design model prototype was implemented in a Finite Element Method (FEM) simulation platform COMSOL Multiphysics [15] in a 2D symmetric plane with the models Piezo Strain Plane for the active element actuation and the model Pressure Acoustic for the pressure waves. The selected mesh has particles with triangular shape and with 300  $\mu\text{m}$  size in a half-sphere shaped environment with 30 cm radius. The simulations were performed with the following settings: fresh water as propagation medium, 20 °C of temperature.

The results show that the transducer exceeded the expected 70 degrees, for both cases. For the 750 kHz the beam spread reaches the 80 degrees with an average pressure level of 155 dB. Considering (8) when the frequency increases, the beam spreading angle should reduce, however this is not verified on these results. In the 1.25 MHz simulation the beam spread overcome the 90 degrees with a higher pressure level around 175 dB at 20 degrees and an average of 165 dB.

Considering the transducer dimensions and the frequencies used, a piston transducer under these conditions should show a beam pattern purely directional.

In conclusion, the simulations results are in accordance with the expected, making this transducer design suitable for implementation.

##### B. Implementation

The transducer was implemented in accordance to the dimensions and characteristics drawn from simulation. The PVDF films were glued using a thin layer of silicone in a curved stainless steel substrate, as showed in Fig 3.

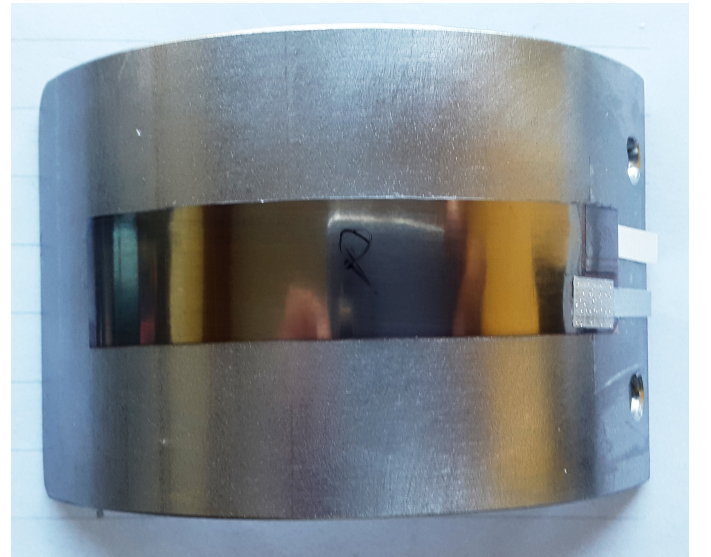


Fig. 3. PVDF films glued to the curved stainless steel substrate.

The electrodes were connected to the conductive wires using aluminum tape and silver paint. For waterproofing, a thin layer of silicone was added on top, as showed in Fig. 4.

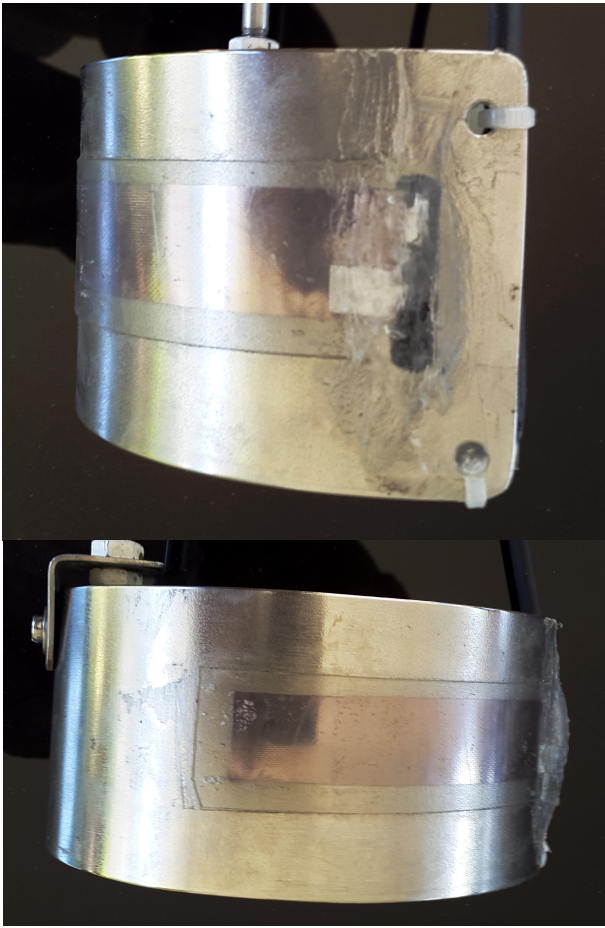


Fig. 4. Final appearance of the transducer.

## V. EXPERIMENTAL SETUP AND RESULTS

The transducer was tested in a fresh water pool with 10 meters long, 5 meters wide and 2 meters deep with water at a temperature around 21°C. To avoid the overlapping of multipath signals the following have been taken into account:

- The emitter and the hydrophone were placed at the pool center aligned in a diagonal line at 50 cm depth, to reduce the probability of receiving reflections, assuming that the hydrophone is directional.
- The signal sent was a sine wave with 20 cycles of 250, 500, 750, 1000, 1250 and 1500 kHz with 10 ms interval between bursts, this way the received echoes do not overlap each other.

Fig. 5 shows a diagram of the experimental setup implemented for the transducer tests. The equipment used was a Signal Generator B&K Precision 4053 amplified by a 5 W Classe B Push-Pull symmetric voltage amplifier with a maximum gain of 12 dB. The hydrophone was a Cetacean Research™ C304XR, with a transducer sensibility of -180 dB, re 1 V/μPa, a linear Frequency Range ( $\pm 3$ dB) of 0.012–1000 kHz and usable Frequency Range ( $\pm 3$ dB) of 0.005–2000 kHz with a 2nd order active band-pass filter from 1 to

2000 kHz with 6 dB gain. The digital oscilloscope PicoScope 4227, 100 MHz, was used to record the measurements.

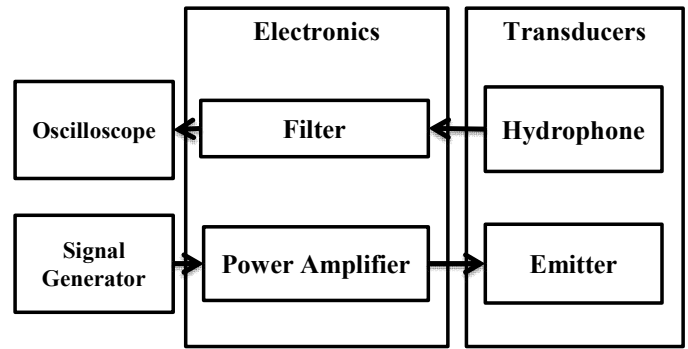


Fig. 5. Experimental setup diagram.

Fig. 6 shows the measured transmitting voltage response (TVR) at 1 meter as a function of the beam spreading angle for 250, 500, 750, 1000, 1250 and 1500 kHz. The graph shows the response to a symmetric axis in XY plane according Fig 1.

The PVDF transducer results were calibrated through the hydrophone sensibility.

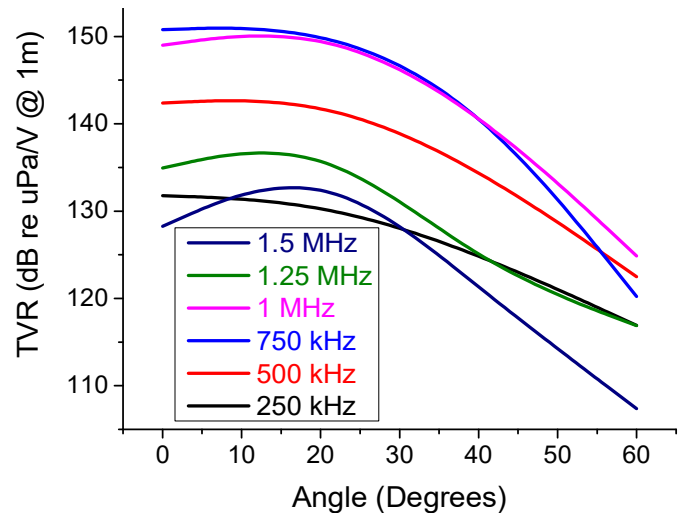


Fig. 6. Unnormalized radiation diagram for various frequencies between 250 kHz and 1.5 MHz.

In terms of angle response, the transducer has a beam wider than the expected 70 degrees and in terms of bandwidth at 1 meter showed a quality factor of 1.5 centered in 755 kHz, demonstrating high bandwidth properties.

Through the simulation it was possible to predict the transducer beam angle for all frequencies and also the increase of pressure levels in the lateral lobes (at 20 degrees) for frequencies above 1 MHz.

Before comparing the simulation results with the experimental ones, is important to remind that the hydrophone only displays a linear behavior ( $\pm 3$  dB) up to 1MHz, therefore to results above 1MHz will be highly affected by the hydrophone sensibility. Another aspect that may cause some differences in the results was the distance, the simulation was

performed with 30 cm, while the tests were performed at 1 m. Considering this aspects we can conclude that the experimental results are in agreement with those obtained in simulations.

Fig. 7 shows the transducer response between 200 kHz and 1.5MHz for 1, 5 and 10 meters distances.

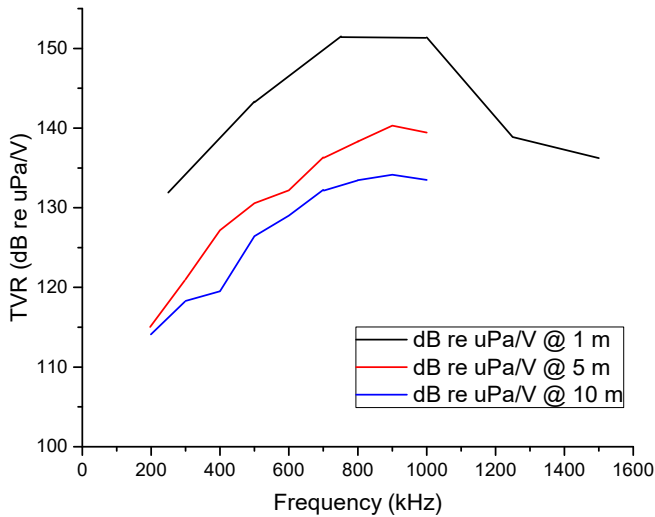


Fig. 7. Frequency response for 1, 5 and 10 meters distance.

The transducer was designed for frequencies up to 1 MHz, but the results show that the transducer is able to operate with frequencies up to 1.5 MHz at short distances. However, it was not possible to do proper measurements at higher distances since, as previous mentioned, the hydrophone sensibility strongly decrease after 1 MHz and at 5 and 10 m it was not enough to capture the acoustic signal.

The results obtained were as expected, and demonstrate a high potential for applications in short-range (up to 10 m) broadband underwater communications since the transducer presents a high bandwidth and beam-width, up to 500 kHz and 70 degrees respectively.

## CONCLUSIONS

The development of a high frequency and wide beam PVDF ultrasound transducer for underwater communications is presented. The transducer has a quality factor of 1.5, centered at 755 kHz with a beam spreading angle larger than 70 degrees. The transducer TVR is higher than 150 dB re uPa/V @ 1m from 750 kHz to 1MHz and a higher than 130 dB re uPa/V @ 1m between 250 kHz and 1.5MHz was measured. When excited with 12V (1MHz) the transducer uses the power of 37.5 mW. The results showed that the developed transducer appears to have the required characteristics of wide band and wide beam to potentially support underwater broadband communications in the band of 250 to 1000 kHz.

## ACKNOWLEDGMENT

This work was co-financed by Programa Operacional Regional do Norte (NORTE2020), through Fundo Europeu de Desenvolvimento Regional (FEDER), Project NORTE-01-0145-FEDER-000032 – NextSea. This work is co-financed by FCT with the reference project UID/EEA/04436/2013, by FEDER funds through the COMPETE 2020 – Programa Operacional Competitividade e Internacionalização (POCI) with the reference project POCI-01- 0145-FEDER- 006941. M. S. Martins thanks FCT for the grant SFRH/BPD/107826/2015.

## REFERENCES

- [1] M. Chitre, S. Shahabudeen, and M. Stojanovic, 'Underwater Acoustic Communications and Networking: Recent Advances and Future Challenges', *Mar. Technol. Soc. J.*, vol. 42, no. 1, pp. 103–116, Mar. 2008.
- [2] D. C. Thompson, M. M. Tentzeris, S. Member, and J. Papapolymou, 'Experimental Analysis of the Water Absorption Effects on RF / mm-Wave Active / Passive Circuits Packaged in Multilayer Organic Substrates', vol. 30, no. 3, pp. 551–557, 2007.
- [3] N. Farr, A. D. Chave, L. Freitag, J. Preisig, S. N. White, D. Yoerger, and F. Sonnichsen, 'Optical Modem Technology for Seafloor Observatories', in *OCEANS 2006*, 2006, pp. 1–6.
- [4] C. H. Sherman and J. L. Butler, *Transducers and Arrays for Underwater Sound*. Springer Science+Business Media, LLC, 2007.
- [5] D. J. Leo, *Engineering Analysis of Smart Material Systems*. Hoboken, NJ, USA: John Wiley & Sons, Inc., 2007.
- [6] P. A. Lewin and P. E. Bloomfield, 'PVDF transducers-a performance comparison of single-layer and multilayer structures', *IEEE Trans. Ultrason. Ferroelectr. Freq. Control*, vol. 44, no. 5, pp. 1148–1156, Sep. 1997.
- [7] M. S. Martins, J. Cabral, S. Lanceros-Mendez, and G. Rocha, 'Effect of the acoustic impedance in ultrasonic emitter transducers using digital modulations', *Ocean Eng.*, vol. 100, pp. 107–116, May 2015.
- [8] A. Seema, K. R. Dayas, and J. M. Varghese, 'PVDF-PZT-5H Composites Prepared by Hot Press and Tape Casting Techniques', vol. 106, no. October 2006, pp. 146–151, 2007.
- [9] N. Yamamoto, Y. Yamashita, Y. Hosono, and K. Itsumi, 'Electrical and physical properties of repled PMN–PT single-crystal sliver transducer', *Sensors Actuators A Phys.*, vol. 200, pp. 16–20, Oct. 2013.
- [10] S. Saitoh, T. Kobayashi, K. Harada, S. Shimanuki, and Y. Yamashita, 'A 20 MHz single-element ultrasonic probe using 0.91Pb(Zn(1/3)Nb(2/3))O(3)-0.09PbTiO(3) single crystal.', *IEEE Trans. Ultrason. Ferroelectr. Freq. Control*, vol. 45, no. 4, pp. 1071–6, Jan. 1998.
- [11] M. Martins, V. Correia, J. M. Cabral, S. Lanceros-Mendez, and J. G. Rocha, 'Optimization of piezoelectric ultrasound emitter transducers for underwater communications', *Sensors Actuators A Phys.*, vol. 184, pp. 141–148, Sep. 2012.
- [12] V. Sencadas, R. Gregorio, and S. Lanceros-Mendez, 'α to β Phase Transformation and Microstructural Changes of PVDF Films Induced by Uniaxial Stretch', *J. Macromol. Sci. Part B*, vol. 48, no. 3, pp. 514–525, May 2009.
- [13] J. B. Babu, G. Madeswaran, R. Dhanasekaran, K. Trinath, A. V. N. R. Rao, N. S. Prasad, and I. R. Abisekaraj, 'Ferroelectric Properties and Transmission Response of PZN-PT Single Crystals for Underwater Communication', vol. 57, no. 1, pp. 89–93, 2007.
- [14] M. Specialties, 'Piezo Film Sensors Technical Manual', 2013. [Online]. Available: <http://www.te.com/usa-en/product-CAT-PFS0003.html>.
- [15] COMSOL Inc., 'COMSOL Multiphysics Modeling Software'. 2016.